Development 134, 3527-3537 (2007) doi:10.1242/dev.002352

Sequential and combinatorial inputs from Nodal, Delta2/Notch and FGF/MEK/ERK signalling pathways establish a grid-like organisation of distinct cell identities in the ascidian neural plate

Clare Hudson*, Sonia Lotito and Hitoyoshi Yasuo

The ascidian neural plate has a grid-like organisation, with six rows and eight columns of aligned cells, generated by a series of stereotypical cell divisions. We have defined unique molecular signatures for each of the eight cells in the posterior-most two rows of the neural plate – rows I and II. Using a combination of morpholino gene knockdown, dominant-negative forms and pharmacological inhibitors, we tested the role of three signalling pathways in defining these distinct cell identities. Nodal signalling at the 64-cell stage was found to be required to define two different neural plate domains – medial and lateral – with Nodal inducing lateral and repressing medial identities. Delta2, an early Nodal target, was found to then subdivide each of the lateral and medial domains to generate four columns. Finally, a separate signalling system along the anteroposterior axis, involving restricted ERK1/2 activation, was found to promote row I fates and repress row II fates. Our results reveal how the sequential integration of three signalling pathways – Nodal, Delta2/Notch and FGF/MEK/ERK – defines eight different sub-domains that characterise the ascidian caudal neural plate. Most remarkably, the distinct fates of the eight neural precursors are each determined by a unique combination of inputs from these three signalling pathways.

KEY WORDS: *Ciona*, Ascidian, Neural patterning, Nodal, Delta, Notch, FGF, MEK, ERK

INTRODUCTION

The central nervous system (CNS) of the *Ciona intestinalis* larva is remarkably similar in overall organisation to, but much simpler than, its vertebrate counterpart. It consists of an anterior sensory vesicle, followed by a narrow neck region, trunk ganglion and tail nerve cord, which are thought to correspond to the forebrain/midbrain (sensory vesicle), hindbrain (neck) and spinal cord (trunk ganglion), respectively (reviewed in Lemaire et al., 2002) [see Dufour et al. for recent advances (Dufour et al., 2006)]. Furthermore, it exhibits gene expression profiles along the anteroposterior and dorsoventral axes that are comparable to the vertebrate neural tube (reviewed in Lemaire et al., 2002). One of the advantages of studying early ascidian development is its relative morphological simplicity. Embryos develop with a fixed cell-cleavage pattern and embryonic blastomeres undergo early fate restriction. This has resulted in well-described cell lineages and fate maps (Cole and Meinertzhagen, 2004; Nicol and Meinertzhagen, 1998a; Nicol and Meinertzhagen, 1988b; Nishida, 1987), which allow the precise identification of cells and the study of cell fate specification events at the level of individual blastomeres; a level of precision not currently accessible in any other chordate model. The recent surge in interest in the *Ciona* model has resulted in the availability of the draft genome (Dehal et al., 2002), extensive EST collections (Satou et al., 2005), a 'virtual' 3D-embryo (Tassy et al., 2006) and the unravelling of the first draft whole-embryo gene regulatory network of a chordate (Imai et al., 2006).

Developmental Biology Unit, Université Pierre et Marie Curie (Paris 6) and CNRS, Observatoire Océanologique, 06230 Villefranche-sur-Mer, France.

*Author for correspondence (e-mail: clare.hudson@obs-vlfr.fr)

Accepted 26 July 2007

We are exploiting the advantages of the *Ciona* embryo to study the generation of cell diversity in the CNS at neural plate stages, when cells are precisely aligned in a grid-like organisation and each cell can be identified (Cole and Meinertzhagen, 2004; Nicol and Meinertzhagen, 1988b; Nishida, 1987). The CNS derives from three of the four blastomere types present at the eight-cell stage, the a-, b- and A-blastomeres. This study concerns the patterning of the A-blastomere-derived part of the nervous system, which emerges at the 64-cell stage following a cell division that generates four notochord and four neural precursors (Fig. 1A). The medial pair of A-line neural precursors (A7.4) form the posterior part of the sensory vesicle and the ventral-most row of cells in the trunk ganglion and tail nerve cord, whereas the lateral cells (A7.8) form the lateral part of the trunk ganglion and tail nerve cord. At the next division, these four neural precursor cells divide along the mediolateral axis to generate one row of eight cells at the early gastrula stage (Fig. 1A). The next division, along the anteroposterior axis, generates two rows of eight cells occupying the posterior-most part of the neural plate. At this time the a- and A-derived neural plate consists of 40 cells aligned in six rows and eight columns (Fig. 1A). Rows of cells are named as rows I to VI, with row I the posterior-most row; columns are named as 1 to 4, with column 4 the most lateral and column 1 the most medial in this bilaterally symmetrical neural plate. The A-neural lineage contributes rows I and II (Fig. 1A). One muscle precursor is also generated from the lateral neural plate at the row I/column 4 position – the A9.31 blastomere (Fig. 1A). This muscle cell forms part of the so-called secondary muscle lineages, which generate the posterior-most larval muscle in the tail (Nicol and Meinertzhagen, 1988a; Nishida, 1990).

We have previously shown that laterally localised Nodal signalling sources participate in patterning the A-line neural plate of *Ciona* embryos across its mediolateral axis (Hudson and Yasuo, 2005). In the absence of Nodal signalling, all lateral neural plate

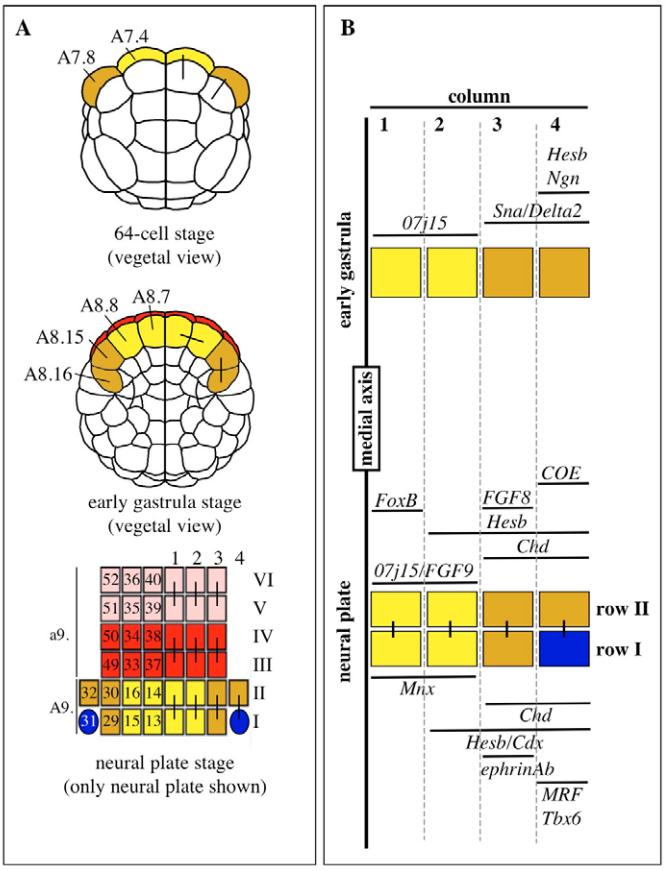

Fig. 1. The cell lineages and gene expression domains of the ascidian CNS. (**A**) Cell lineages of the CNS. Embryonic stages are indicated below the drawings. Blastomere names are indicated on the left half of the drawings. At the neural plate stage (neural plate shown only), blastomere names should be prefixed with an a9. for a-line and A9. for A-line, as indicated. Bars connecting blastomeres on the right half of the drawings indicate a sister cell relationship. A-line lineages are shown in yellow for medial precursors and tan for lateral precursors, with the secondary muscle precursor coloured in blue. a-line lineages are indicated in red (sensory vesicle) and pink (anterior epidermis and pharynx; because of the cell arrangement, these cells are considered part of the neural plate although they do not contribute to the CNS). In addition, cells from the b-line, positioned lateral to the A- and a-line neural plate, contribute to the dorsal part of the CNS (data not shown). The same colour code is used in all subsequent figures. At the neural plate stages, cells are organised into four columns (1-4) and six rows (I-VI), as indicated. (**B**) Schematic representation of the gene expression profiles in A-line neural lineages at early gastrula and neural plate stages. The right-hand-side A-line neural blastomeres of the bilaterally symmetrical embryo are represented; the position of the medial axis is indicated on the left. Bars above and below the schematics indicate gene expression for the markers used in this study (row II above, row I below). Position of the columns and rows are indicated (top and right). Sna, Snail; 07j15, cicl07j15; FGF8, FGF8/17/18; Chd, Chordin; FGF9, FGF9/16/20.

fates (columns 3 and 4) are lost and lateral cells appear to adopt a medial (columns 1 and 2) neural plate-like fate. It is not known, however, how the differential fates in columns 3 and 4 of the lateral neural plate, or columns 1 and 2 of the medial neural plate, become distinguished, nor how cells adopt different fates along the anteroposterior axis (row I versus row II). Here, we have investigated the involvement of three distinct signalling pathways in A-line neural plate patterning along the mediolateral and anteroposterior axes, and show that combinatorial inputs from Nodal-, Delta2- and ERK1/2-based signalling can account for the eight cell identities defined by differential gene expression.

MATERIALS AND METHODS

Embryo culture, manipulation, morpholinos and injection/electroporation constructs

Adult *Ciona intestinalis* were purchased from the Roscoff Marine Biological Station (Roscoff, France). Blastomere names, lineages and fate mapping are as described (Conklin, 1905; Cole and Meinertzhagen, 2004; Nicol and Meinertzhagen, 1988a; Nicol and Meinertzhagen, 1988b; Nishida, 1987). Embryo culture, microinjection and the *dnDel2* injection construct have been described previously (Hudson et al., 2003; Hudson and Yasuo, 2006). *Nodal*-MO (morpholino oligonucleotide) and *Delta2*-MO were purchased from GeneTools LLC and have been described elsewhere (Hudson and Yasuo, 2005; Hudson and Yasuo, 2006), except that *Delta2*-MO was injected in a slightly higher concentration of 0.2 mM, rather than 0.125 mM, in some experiments. pRN3-dnFGFR was generated from the EST clone *citb040h06*. A DNA fragment encoding the extracellular and transmembrane domains was PCR-amplified with a primer set, 5′-GGCCAGATCTACCATGATA-CAACTACAAAATACG-3′ and 5′-GCGCGCGGCCGCTCACAAACG-GGGAGGATCTTTATTT-3′, and subcloned into the *Bgl*II and *Not*I sites of pRN3. *dnFGFRc* mRNA was injected at a concentration of 1 μg/μl. Electroporations were carried out as previously described (Corbo et al., 1997; Bertrand et al., 2003). The FOG::Delta2 construct is similar to that described previously (Pasini et al., 2006) except that the construct we used, which was a gift from A. Pasini (IBDML, Marseille, France), lacks the UTRs of the *Delta2* gene of *Ciona intestinalis* (*Ci-Delta2*).

In situ hybridisation and immunohistochemistry

dpERK1/2 immunohistochemistry, in situ hybridisation and Hoechst staining were carried out as previously described (Hudson and Yasuo, 2005; Hudson and Yasuo, 2006; Picco et al., 2007; Wada et al., 1995). Dig-labelled RNA probes were synthesised from the following cDNA clones derived from the Kyoto Gene Collection plates or previously described: *Ci-Actin*, *Ci-Chordin*, *Ci-Delta2*, *Ci-FGF8/17/18*, *Ci-FGF9/16/20*, *Ci-HB9/Mnx* [re-named *Ci-Mnx* (Imai et al., 2006)], *Ci-Hesb* and *Ci-Snail* (Hudson and Yasuo, 2005); *Ci-Cdx*, *Ci-COE*, *Ci-FoxB* and *Ci-Ngn* (Imai et al., 2006); *Ci-ephrinAb* (Imai et al., 2004); *cicl007j15* (Fugiwara et al., 2002; Satou et al., 2005); *Ci-MRF* (Meedel et al., 2007); *Ci-Tbx6b* (Takatori et al., 2004); and *Ci-Otx* (Hudson and Lemaire, 2001).

Inhibitor treatments and establishing the approximate timing of penetration

SB431542 (Tocris), U0126 (Calbiochem) and DAPT (Calbiochem) treatments in *Ciona* have been described previously (Hudson et al., 2003; Hudson and Yasuo, 2005; Hudson and Yasuo, 2006). Prior to carrying out the experiments described in this study, we wanted to have some idea of how long these chemical inhibitors take to penetrate and act upon the expression of the target genes. *Ci-Otx* expression in a6.5 and b6.5 blastomeres at the 44-cell stage has been identified as a direct target of FGF9/16/20 acting via MEK/ERK (Bertrand et al., 2003; Hudson et al., 2003). *Ci-FGF9/16/20* is expressed from the 16-cell stage, ERK1/2 is activated in the a6.5 and b6.5 blastomeres during the latter half of the 32-cell stage and *Ci-Otx* is expressed in these cells at the 44-cell stage, approximately 20-30 minutes after the onset of ERK1/2 activation (Bertrand et al., 2003; Hudson et al., 2003). Thus, there is a lag between transcription of the ligand gene (*FGF9/16/20*), detectable activation of the pathway (dpERK1/2) and the readout in target gene expression (*Ci-Otx*), which should be considered when trying to establish how long a pharmacological reagent takes to penetrate and act. We found that embryos need to be placed in the MEK/ERK inhibitor, UO126 (Duncia et al., 1998; Favata et al., 1998), 20-30 minutes prior to fixation at the 44-cell stage, which corresponds to the early 32-cell stage, in order to completely inhibit detectable *Ci-Otx* expression (see Fig. S1 in the supplementary material). This is just prior to detectable ERK1/2 activation and suggests that UO126 can penetrate the embryo and act very quickly.

Similarly, we placed embryos in an inhibitor of gamma-secretase, DAPT (Geling et al., 2002), at different time points starting from the 44-cell stage and analysed expression of a potential direct target of Delta2/Notch signalling, *Ci-Hesb*, at the early gastrula stage. DAPT treatment strongly downregulated *Ci-Hesb* expression when applied 30-40 minutes prior to fixation (see Fig. S1 in the supplementary material). Finally, we tested how long SB431542, a pharmacological inhibitor of ALK4/5/7 (Inman et al., 2002), might take to block *Ci-Delta2* expression, which is the earliest identified target of Nodal signals. SB431542 had to be applied to embryos approximately 40 minutes prior to fixation in order to downregulate *Ci-Delta2* expression at the 64-cell stage. We conclude, given that there should be a time lag between expression of the ligand and onset of target gene transcription, that all of these inhibitors penetrate and act in a reasonably short period of time.

RESULTS

Gene expression profiles in the ascidian neural plate

We have previously described a collection of gene expression profiles that we used as molecular markers to study neural plate patterning (Fig. 1B) (Hudson and Yasuo, 2005). In this study, additional genes were included, which were found by searching the EST/in situ data banks 'Ghost' and 'ANISEED' (e.g. Imai et al., 2004; Tassy et al., 2006; Satou et al., 2005). The *Ciona intestinalis Neurogenin* gene (*Ci-Neurogenin*; *Ci-Ngn*) encodes a basic helix-loop-helix (bHLH) transcription factor and its expression was restricted to the lateral-most A-line neural blastomere, A8.16, at the early gastrula stage (Fig. 1B, Fig. 2) (Imai et al., 2004; Imai et al., 2006). *cicl007j15* encodes a protein with similarity to a regulator of G-protein signalling. Expression was restricted at the early gastrula stage to the medial four cells (columns 1 and 2) of the A-line neural lineage (Fig. 1B, Fig. 2). This supports previous evidence that medial and lateral cells are undergoing different developmental programs by the early gastrula stage, with *Ci-Snail* and *Ci-Delta2* only in the lateral cells (Fig. 1B) (Hudson and Yasuo, 2005). This gene expression profiling further revealed that, by the early gastrula stage, column 3 (A8.15) and column 4 (A8.16) precursors become distinguishable, with expression of *Ci-Ngn* and *Ci-Hesb* only in A8.16 (Fig. 1B, Fig. 2) (Hudson and Yasuo, 2006; Imai et al., 2006). Thus, by the early gastrula stage the A-line neural cells can be divided into three domains in terms of gene expression (Fig. 1B).

At the neural plate stage, *cicl007j15* is expressed in the medial cells of row II (Fig. 1B, Fig. 2) (Fujiwara et al., 2002). *Ci-ephrinAb* encodes a GPI-anchored ephrin ligand (Satou et al., 2003a) and we detected expression in row I/column 3 (A9.29) of the neural plate (Fig. 1B, Fig. 2). *Ci-COE* encodes a transcription factor of the Collier/Olf/EBF family (Satou et al., 2003b) and its expression was detected in row II/column 4 (A9.32) (Fig. 1B, Fig. 2) (Imai et al., 2006). We also included two markers of muscle fate, *Ci-Tbx6b* and *Ci-MRF*, encoding transcription factors of the T-box and bHLH classes, respectively; these are detectable in row I/column 4 (A9.31) (Fig. 1B, Fig. 2) (Meedel et al., 2007; Takatori et al., 2004). These expression profiles indicate that in the neural plate, soon after each division, individual blastomeres undergo different developmental programmes. In the posterior two rows of the neural plate, we can thus define eight expression domains corresponding to the eight different cells (Fig. 1B). In row I, the expression domains are as follows: column 1 (*Mnx*), column 2 (*Mnx*, *Hesb* and *Cdx*), column 3 (*Hesb*, *Cdx*, *Chordin* and *ephrinAb*, of which *ephrinAb* is specific to this cell) and column 4 (*Hesb*, *Cdx*, *Chordin*, *MRF* and *Tbx6b*, of which *MRF* and *Tbx6b* are specific to this cell). In row II, the expression domains are as follows: column 1 (*FGF9/16/20*, *cicl007j15* and *FoxB*, of which *FoxB* is specific to this cell), column 2 (*FGF9/16/20*, *cicl007j15* and *Hesb*), column 3 (*Hesb*, *Chordin* and *FGF8/17/18*, of which *FGF8/17/18* is specific to this cell) and column 4 (*Hesb*, *Chordin* and *COE*, of which *COE* is specific for this cell). Thus, each of the eight blastomeres in the posterior neural plate exhibits a unique combination of gene expression profiles, which can be used as a molecular signature for each cell identity and, in particular, a cell-specific marker has been identified for each of

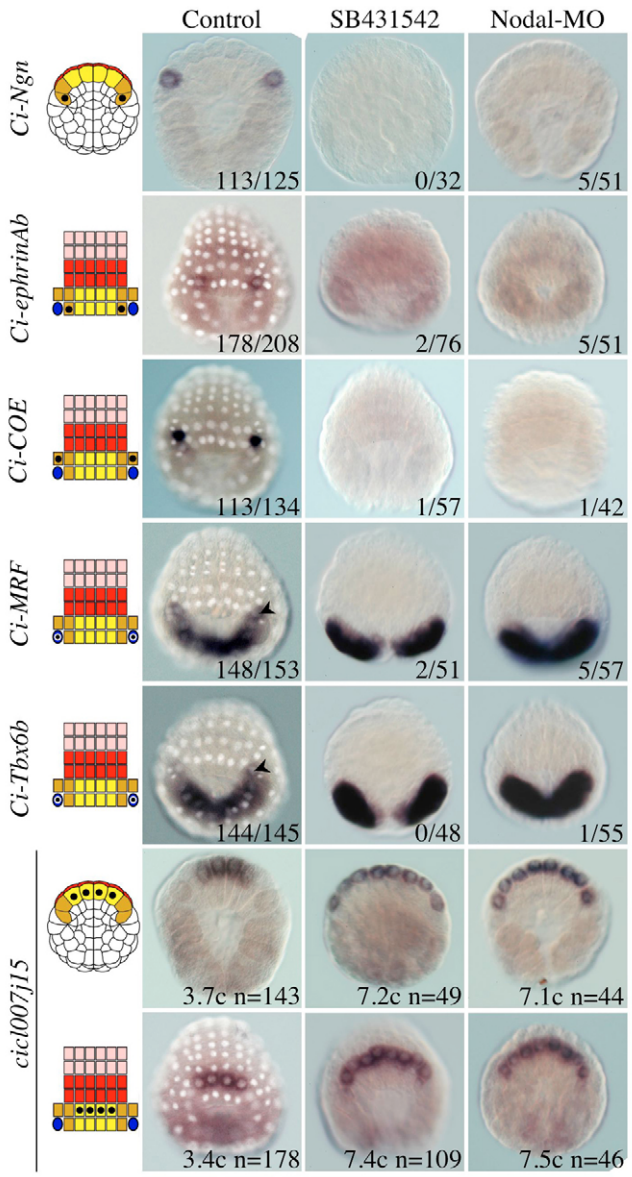

Fig. 2. Expression of various gene markers of the A-line neural cells following inhibition of Nodal signals. Embryo treatment is indicated above the panels and the marker analysed to the left of the panels. For control neural plate-stage embryos, nuclei are labelled with Hoechst (white) to allow the easy identification of individual cells. For this and subsequent figures, black dots on the schematics mark blastomeres expressing each given gene and, unless otherwise stated in the text, the vast majority of embryos exhibited bilateral staining. Expression of *Ci-MRF* and *Ci-Tbx6b* in A9.31 is indicated by an arrowhead on the right-hand side. For lateral markers, numbers indicate any expression over the total number of embryos analysed. For the medial marker *cicl007j15*, numbers indicate the mean number of cells (c) per embryo expressing a given gene. n, total number of embryos analysed.

the lateral four cells: *COE*, *FGF8/17/18*, *MRF/Tbx6b* and *ephrinAb* (Fig. 1B). We next addressed how each cell identity in the posterior neural plate, characterised by these distinct profiles of gene expression, is generated.

Lateral versus medial neural plate fate specification

Each of these additional molecular markers behaved as predicted from previous work when Nodal signalling was inhibited: medial markers were expanded at the expense of lateral markers (Hudson and Yasuo, 2005; Imai et al., 2006). Nodal signalling was blocked by treatment with a pharmacological inhibitor of ALK4/5/7, SB431542, or by injecting a morpholino oligonucleotide against *Ci-Nodal* (Fig. 2). Expression of the lateral neural plate markers *Ci-Ngn*, *Ci-ephrinAb*, *Ci-COE*, *Ci-MRF* and *Ci-Tbx6b* was inhibited, whereas that of the medial marker *cicl007j15* was expanded into the lateral cells both at the early gastrula and neural plate stages. A reduction in *Ci-COE* and *Ci-Ngn* expression at the late gastrula stage has previously been reported by quantitative reverse transcriptase (RT)-PCR or in situ hybridisation analysis following Nodal inhibition (Imai et al., 2006). These data provide further evidence that Nodal signalling is required for the formation of all lateral A-line neural plate fates of columns 3 and 4, and shows that expansion of medial fates into the lateral A-line neural precursors occurs as early as the early gastrula stage.

We next addressed the timing of Nodal signalling required for lateral versus medial neural plate fates by placing embryos in SB431542 at different developmental time points. We analysed, at the early gastrula stage, *Ci-Snail* expression as a general lateral marker, *Ci-Ngn* expression as an A8.16 marker, and *cicl007j15* as a medial marker. We found that at around the 64- to 76-cell stage of development, expression of all three genes became insensitive to SB431542 treatment (Fig. 3). SB431542 can penetrate embryos and act within at least 40 minutes (see Fig. S1C in the supplementary material and see Materials and methods), indicating that, by the early gastrula stage at the latest, Nodal-mediated lateral versus medial fates are determined. It has been proposed previously that the lateral-most cell, A8.16, might adopt a distinct fate to its more medial sister cell, A8.15, due to its prolonged contact with Nodal-expressing b-line cells (Hudson and Yasuo, 2005; Imai et al., 2006). However, because *Ci-Snail* and *Ci-Ngn* exhibit a similar temporal dependency to Nodal signals, it is unlikely that this is the case and rather suggests that Nodal mediates only medial versus lateral fate specification and that other mechanisms subsequently act to further pattern the lateral columns.

Delta2 is required for column 4 gene expression

We have shown previously that Delta2/Notch signalling acts in a relay of Nodal signalling during the induction of the secondary notochord fate (Hudson and Yasuo, 2006). *Ci-Delta2* is expressed from the late 64-cell stage in A7.6, b7.9 and b7.10, with weak expression also observed occasionally in A7.8 (Fig. 4A) (Hudson and Yasuo, 2006). A7.6 and b7.10 blastomeres are in direct contact with the A7.8 blastomere, the founder of neural plate columns 3 and 4 (Fig. 1A). This expression of *Ci-Delta2* persists during the cell division of A7.8 into A8.15 and A8.16 at the 76-cell stage, with the *Ci-Delta2*-expressing cells remaining in contact only with A8.16, the column 4 precursor (Fig. 4A). We investigated whether Delta2/Notch signalling plays a role during patterning of the A-line-derived neural plate using a morpholino oligonucleotide against *Delta2* (*Del2*-MO), a dominant-negative version of Delta2 lacking the intracellular domain (dnDel2) and DAPT, a pharmacological

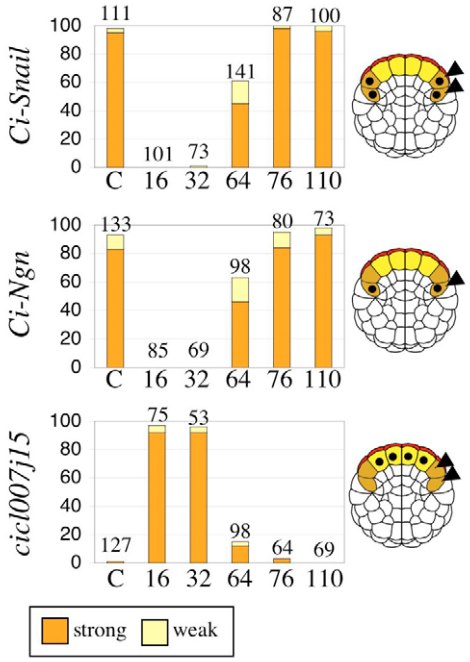

Fig. 3. Temporal dependency of early gastrula-stage A-neural markers to Nodal signal inhibition. Markers analysed are indicated on the left of the graphs. Graphs show the percentage of embryos with strong or weak expression in the lateral neural precursors (marked with arrowheads). Scoring was as follows: *Ci-Snail*, strong = at least two cells positive, weak = one cell positive or very weak expression in one to four cells; *Ci-Ngn*, strong = at least one cell positive, weak = at least one blastomere showing very weak expression; *cicl007j15*, strong = at least two lateral cells positive, weak = one lateral cell positive or weak expression in one to four lateral cells. For *cicl007j15*, only embryos with expression in one to four medial cells were included in the analysis. Numbers shown above the bars indicates the total number of embryos analysed. On the *x*-axis is shown the developmental time point when embryos were placed in inhibitor: C, control; 16, 32, 64, 76, 110 = cell stage.

inhibitor of gamma-secretase, an enzyme required for Notch receptor processing. These reagents have previously been shown to inhibit Delta2/Notch signalling in *Ciona* embryos (Hudson and Yasuo, 2006).

We first analysed the effect on A-line neural patterning at the early gastrula stage (Fig. 4B). Expression of the general lateral markers *Ci-Snail* and *Ci-Delta2* in A8.15 and A8.16 cells was not affected by inhibition of Delta2/Notch signalling. Similarly, the medial marker *cicl007j15* was not expanded. Thus, Delta2/Notch signalling is not required for medial versus lateral neural plate fates. However, expression of *Ci-Ngn* in the most-lateral cell, A8.16, was lost. This is consistent with our previous observation that *Ci-Hesb* expression in A8.16 is Delta2/Notch-dependent (Hudson and Yasuo, 2006) and suggests that Delta2 might be required specifically for column 4 fates during the patterning of the A-line neural plate.

The role of Delta2/Notch was further addressed by analysing gene expression at the neural plate stage (Fig. 5; Fig. S2 in the supplementary material). As expected, expression of *Ci-Hesb*, which is a target of Delta2/Notch at early gastrula stages, was lost following Delta2/Notch inhibition. However, *Ci-Chordin*, which is also broadly expressed in the lateral neural plate, was not

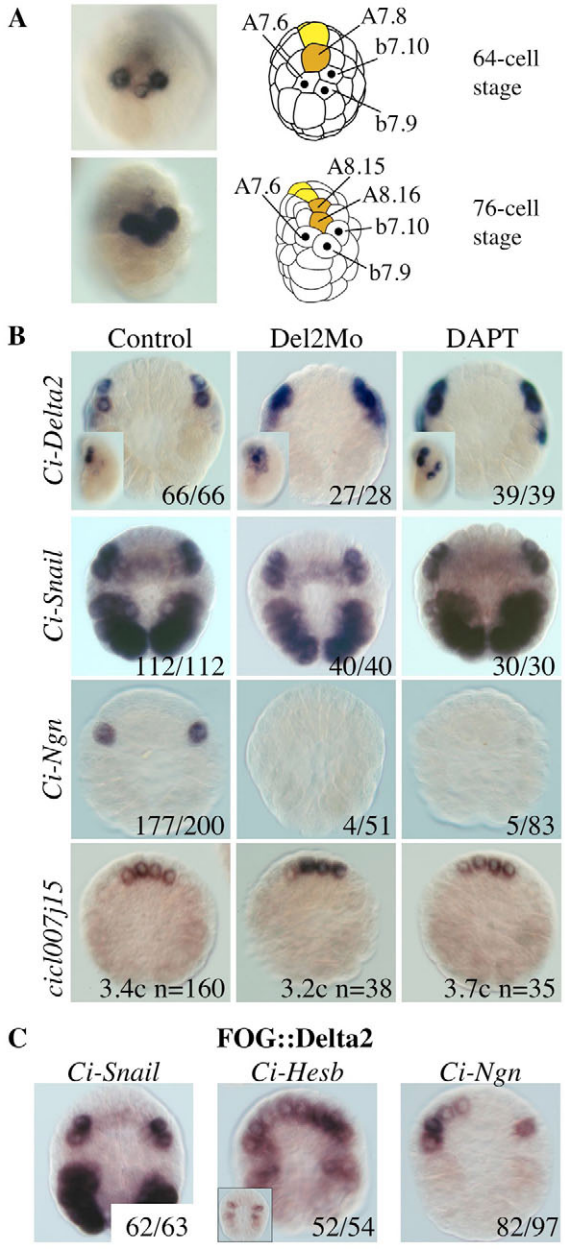

Fig. 4. Expression of A-line neural markers at the early gastrula stage following Delta2/Notch inhibition or ectopic activation. (**A**) Expression of *Ci-Delta2* at the 64- and 76-cell stages. Embryos and schematics are shown in lateral view with the vegetal pole to the left. *Ci-Delta2*-expressing blastomeres surround A7.8, the founder cell of columns 3 and 4, at the 64-cell stage, and surround A8.16, the precursor cell of column 4, at the 76-cell stage. Blastomere names are indicated. (**B**) Expression of markers, indicated on the left, at the early gastrula stage following the treatments indicated above the panels. For lateral markers, numbers indicate any expression seen in A-line neural cells over the total number of embryos analysed. The inserts for *Ci-Delta2* expression are lateral views of embryos, showing that expression is slightly but consistently upregulated following Delta2/Notch inhibition, particularly in b-line cells. For *cicl007j15*, numbers indicate the mean number of positive cells (c) per embryo; n, total number of embryos analysed. Similar results were observed with dnDel2 injection (*Ci-Snail*, 35/35; *Ci-Ngn*, 5/48; *cicl007j15*, 3.2c; *n*=24). (**C**) Expression of markers, shown above the panels, following *FOG::Delta2* electroporation. Numbers indicate: for *Ci-Snail*, the number of embryos showing expression represented by the panel over the total number of embryos analysed; for *Ci-Hesb* and *Ci-Ngn*, the number of embryos showing ectopic expression in A-line neural cells over the total number of embryos analysed. Ectopic expression of *Ci-Hesb* and *Ci-Ngn* was also sometimes observed in additional vegetal cells (data not shown). The insert on the bottom right of *Ci-Hesb* panel shows expression of *Ci-Hesb* in a control embryo.

affected. Similarly, *Ci-FGF8/17/18* and *Ci-ephrinAb*, which are specifically expressed in column 3, were still expressed in the majority of embryos following Delta2/Notch inhibition. This shows that Delta2/Notch signalling is not generally required for lateral neural plate fates. Consistently, *Ci-Mnx* and *Ci-FGF9/16/20* were not expanded into the lateral neural plate following Delta2/Notch inhibition. However, genes that are specifically expressed in column 4, such as *Ci-COE* in row II/column 4 (A9.32), and *Ci-MRF* and *Ci-Tbx6b* in row I/column 4 (A9.31), were Delta2/Notch-dependent (Fig. 5; Fig. S2 in the supplementary material). Loss of secondary muscle fate was confirmed by analysing *Ci-Actin* expression in the A8.16 lineage at the neurula stage in embryos treated with cytochalasin B from the early gastrula stage, a treatment that allows analysis of late marker expression in terms of lineages (e.g. Hudson and Yasuo, 2005). Thus, inhibition of Delta2/Notch results in the specific loss of column 4 identity.

Delta2/Notch signalling is acting upon the column 4 precursor (A8.16)

Loss of column 4 fates following inhibition of Delta2/Notch signalling became apparent at the early gastrula stage with loss of *Ci-Hesb* and *Ci-Ngn* in A8.16. In order to address when Delta2/Notch signalling was required to establish column 4 fates, we placed embryos in DAPT inhibitor at different developmental time points and analysed *Ci-COE* and *Ci-MRF* expression at the neural plate stage (Fig. 6). Expression of *Ci-MRF*, *Ci-Actin* and *Ci-COE* at neural plate stages was not affected by DAPT treatment from the 76-cell stage onwards, coinciding with the stage at which the column 4 precursor (A8.16) is formed. Because DAPT can penetrate and block target gene expression within 30-40 minutes (see Fig. S1B in the supplementary material), well within the cell cycle of A8.16, we conclude that Delta2/Notch is acting upon A8.16 and that, once specified, A8.16 generates two distinct daughter cells (marked by *Ci-COE* and *Ci-MRF*) along the anteroposterior axis in a Notch-independent manner.

Overexpression of Delta2 can promote ectopic column 4 identity

We have shown that Delta2/Notch signalling is required for column 4 fates. In order to address whether Delta2 is sufficient to promote column 4 fates, we overexpressed *Ci-Delta2*. This was carried out using an electroporation construct, *FOG::Delta2*, in which the FOG promoter is placed upstream of *Ci-Delta2*, driving its expression in all animal cells from the 16-cell stage onwards (Pasini et al., 2006). Animal cells are in contact with all the A-line neural precursors up to and including gastrula stages. At the early gastrula stage, we analysed expression of *Ci-Hesb*, *Ci-Ngn* and *Ci-Snail* (Fig. 4C). Following *FOG::Delta2* electroporation, expression of *Ci-Hesb* was observed throughout the A-line neural cells in all columns (column 4, 98%; column 3, 93%; column 2, 89%; column 1, 89%), suggesting that all A-line neural cells received a Delta2/Notch signal

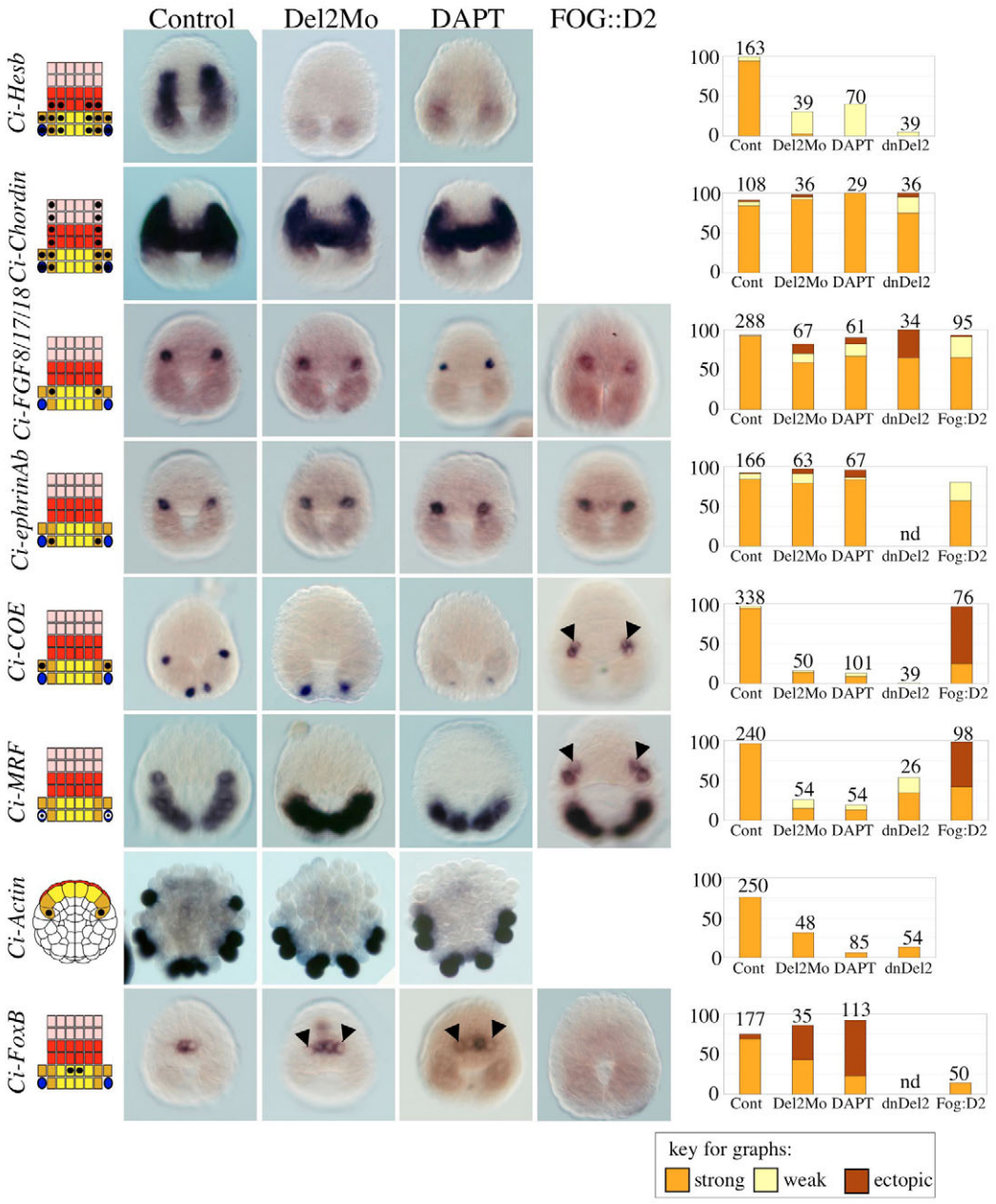

Fig. 5. Expression of various neural plate markers following Delta2/Notch inhibition or ectopic expression. The marker analysed is indicated on the left and embryo treatment is indicated above the panels. Graphs show the percentage of embryos with ectopic, strong or weak expression according to the key indicated below. The same key is used for all subsequent figures. For *Ci-Hesb* and *Ci-Chordin*, 'weak' means reduced expression compared with the majority of controls. For the remaining markers, 'strong' means at least one A-line neural precursor cell with strong expression and 'weak' means at least one cell with downregulated expression. Occasionally, following disruption of Delta2/Notch signalling, ectopic expression was seen for *Ci-FGF8/17/18* and *Ci-ephrinAb*. This ectopic expression appeared in column 4. Following *FOG::Delta2* electroporation (abbreviated to FOG::D2), *Ci-FGF8/17/18* exhibited frequent unilateral expression. Of those scored positive, 49% expressed *Ci-FGF8/17/18* on one side only (compared with 9% of control embryos from the same batches). Ectopic expression of *Ci-COE* following *FOG::Delta2* electroporation appeared in column 3 (A9.30) in the majority of cases (see text for details) with 54% of these cases exhibiting unilateral A9.30 expression and 46% bilateral. Ectopic expression of *Ci-MRF* was observed only in column 3 (A9.29). Of those exhibiting ectopic expression, 66% had column 3 (A9.29) expression on one side only. In most cases, column 3 (A9.29) expression of *Ci-MRF* appeared slightly weaker than the expression in column 4 (A9.31). For *Ci-FoxB*, expression in both control and treated embryos was frequently (around half of those scored positive) observed on one side only. Arrowheads point to ectopic expression on the panels.

under these experimental conditions. Similarly, ectopic *Ci-Ngn* expression was observed, although expression appeared more readily in column 3 compared with columns 1 and 2 (column 4, 100%; column 3, 84.5%; column 2, 30%; column 1, 35%). Consistent with the specific requirement of Delta2 for column 4 fates, the general lateral neural marker, *Ci-Snail*, was not ectopically

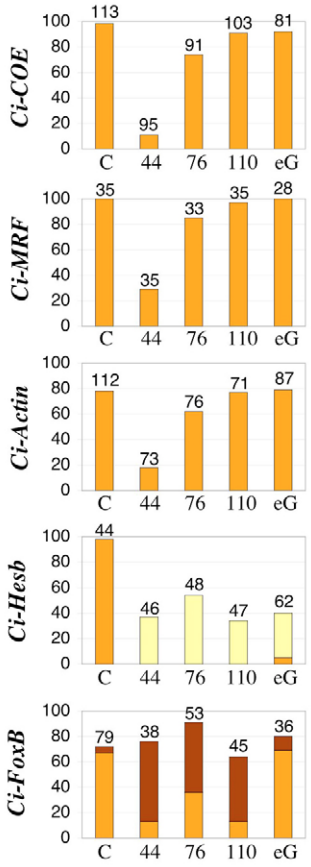

Fig. 6. Analysis of neural plate markers following DAPT treatment at different embryological time points. Graphs show the percentage of embryos with strong, weak or ectopic expression. Scoring was carried out as indicated for Fig. 5. Numbers shown above the bars indicate the total number of embryos analysed. On the *x*-axis is shown the developmental time point when embryos were placed in DAPT inhibitor: C, control; 44, 76, 110 = cell stage; eG, early gastrula stage.

expressed following Delta2 overexpression, showing that Delta2 cannot promote general lateral fates.

We next analysed markers of column 3 (*Ci-Fgf8/17/18* and *Ci-ephrinAb*) and column 4 (*Ci-MRF* and *Ci-COE*) at neural plate stages in *FOG:Delta2*-electroporated embryos. We found that *Ci-COE* was expressed ectopically in row II/column 3 (A9.30; 71%), with expression in columns 2 or 1 rarely observed (4 and 7%, respectively). Under these conditions, a row I/column 4 marker, *Ci-MRF*, was also ectopically expressed in row I/column 3 (A9.29) in 56% of embryos and never in columns 1 and 2. On the other hand, the column 3 markers *Ci-Fgf8/17/18* and *Ci-ephrinAb* appeared slightly downregulated compared with control embryos (Fig. 5).

These data show that Delta2 specifically promotes column 4 identity. It also shows that, at neural plate stages, the competence to express column 4 markers in response to Delta2 is restricted to columns 3 and 4, which previously received a Nodal signal.

Later Delta2/Notch activity is involved in distinguishing column 1 versus column 2 fates

From the 110-cell stage, *Ci-Delta2* is expressed in column 3 and 4 precursors (A8.15 and A8.16, respectively), with column 3 precursors being in direct contact with column 2 precursors (Fig. 4B) (Hudson and Yasuo, 2005). We therefore addressed whether Delta2/Notch might be playing an additional patterning role; in particular, patterning between column 1 and 2. At the neural plate stage, *Ci-Hesb* is expressed in columns 2-4, but not in column 1 (Fig. 5) (Hudson and Yasuo, 2005). On the other hand, *Ci-FoxB* specifically marks the row II/column 1 blastomere (A9.14) (Moret et al., 2005). Both of these markers were found to be sensitive to Delta2/Notch signal inhibition, with *Ci-Hesb* expression being lost and *Ci-FoxB* expression expanded into row II/column 2 (A9.16) (Fig. 5). Conversely, overexpression of *Ci-Delta2* suppressed *Ci-FoxB* expression (Fig. 5). Treatment of embryos with DAPT at different developmental time points revealed that this Delta2/Notch-mediated patterning event takes place later than that for column 4 specification (Fig. 6). This suggests that a later Delta2/Notch signal is required to promote column 2 (*Ci-Hesb* expression) and repress column 1 (*Ci-FoxB* expression) identity in column 2 cells, at least in row II.

Taken together, our results suggest that Delta2/Notch acts to subdivide the neural plate into four columns, with early Delta2/Notch involved in subdividing column 3 and 4 fates in the lateral domain and later Delta2/Notch subdividing column 1 and 2 fates in the medial domain.

Differential FGF/MEK/ERK signals between row I and row II neural plate cells are required for their differential fate specification

Nodal and Delta2/Notch signalling can explain fate differences along the mediolateral axis of the neural plate, but not those along the anteroposterior axis. We therefore considered other candidate signalling pathways. Extracellular-signal-regulated kinase 1/2 (ERK1/2) is a part of an evolutionary conserved signalling cascade acting downstream of receptor tyrosine kinases (RTKs), which are activated by ligands such as FGF. Antibodies against the dual phosphorylated form of ERK1/2 (dpERK1/2) can be used to visualise the pattern of ERK1/2 activation during *Ciona* development (e.g. Yasuo and Hudson, 2007). During neural plate stages, we found that ERK1/2 was differentially activated between row I and row II. Soon after the division of A-line neural plate precursors into row I and row II, at the stage when the entire neural plate consists of four rows of cells, ERK1/2 activation was detected in row I cells, but not in row II cells, and this pattern was maintained until the neural plate consisted of six rows of cells (Fig. 7A). Activation of ERK1/2 was also observed in the a-line precursors of row III. These data are consistent with observations in *Halocynthia* (Nishida, 2003) and suggest that differential ERK1/2 activation between row I and row II cells might be playing a role during patterning of the neural plate along the anteroposterior axis.

In order to address this possibility, we placed embryos in UO126, a pharmacological inhibitor of MEK, which is a kinase required for ERK1/2 activation, at the early gastrula stage. The early gastrula stage is approximately 30 minutes before A-line neural precursors divide into rows I and II. We found that all markers of row I, including *Ci-MRF*, *Ci-Tbx6b*, *Ci-Actin*, *Ci-ephrinAb*, *Ci-Mnx* and *Ci-Cdx*, were lost following inhibition of the MEK/ERK pathway (Fig. 7B, Table 1). By contrast, row II markers were expanded into row I (Fig. 7C; Table 1). This was particularly striking in the lateral cells with an almost complete transformation of row I cells into a row II-like fate, as judged by ectopic expression of *Ci-FGF8/17/18* in row I/column 3 (A9.29) and *Ci-COE* in row I/column 4 (A9.31). A similar transformation took place in the medial cells, although the ectopic expression of row II markers in row I was sometimes weaker than in row II. Importantly, ectopic expression of row II markers in

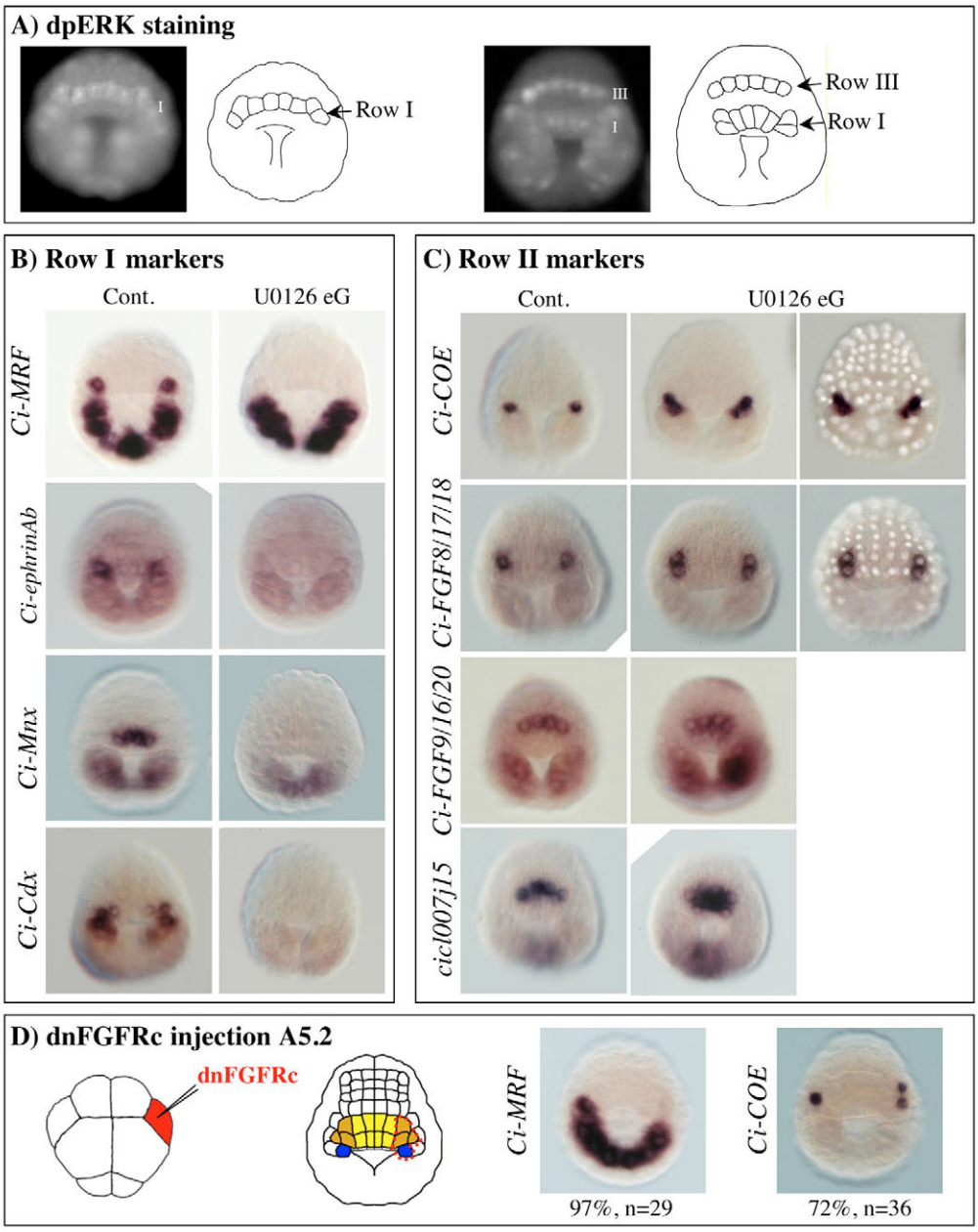

Fig. 7. FGF/MEK/ERK activity is required for row I versus row II fates. (**A**) Activation of ERK1/2 visualised by dpERK1/2 antibody staining. The schematics indicate the neural plate cells positive for ERK1/2 activation, with the rows of cells indicated. The cell outlines were estimated using the ERK staining image and a Hoechst-stained image of the same embryo (data not shown). The embryo on the left contains four rows of cells in the neural plate. At this stage, weak ERK1/2 activation can also be seen in the row III/IV precursors, which are not visible in the panel because of the orientation of the embryo. (**B**) Expression of row I markers following UO126 treatment from the early gastrula stage. *Ci-Cdx* is expressed in A9.31, A9.29 and A9.15 in control embryos (Imai et al., 2006). (**C**) Expression of row II markers following UO126 treatment from the early gastrula stage. Hoechst staining, shown on the right for *Ci-COE* and *Ci-FGF8/17/18*, confirms that ectopic expression in row I was seen in column 4 and column 3, respectively. (**D**) Injection of *dnFGFRc* mRNA into the A5.2 blastomere on the right-hand side. Descendants of A5.2 include those circled in red on the neural plate schematic. (Right) Numbers below the figures show the percentage of embryos that the panels represent and the total number of embryos analysed. Cont., control.

row I was observed only in the same column as the expression normally observed in row II. This indicates that inhibition of MEK/ERK from the early gastrula stage affects only anteroposterior patterning and that mediolateral positional information remains intact in these embryos. Finally, by placing embryos in UO126 at different developmental time points and analysing *Ci-COE* and *Ci-MRF* expression, we found that segregation of these cell types became refractory to MEK inhibition at around the time that A-line neural precursors had divided into row I and row II (Fig. 8).

FGF9/16/20 is expressed in the A-line neural precursors from the 64-cell stage until the mid-gastrula stages, making it a good candidate for the signal responsible for ERK activation in row I (Imai et al., 2002) (our unpublished data). However, we could not address the role of FGF9/16/20 during posterior neural plate patterning because this ligand is required earlier in development for the induction of *Ci-Nodal* expression in the lateral b-line cells at the 32-cell stage and Ci-Nodal is required for mediolateral patterning (Hudson and Yasuo, 2005). In order to address whether FGF signals were required for the differential specification of row I and row II, we injected a dominant-negative FGF receptor (dnFGFRc) into A5.2 at the 16-cell stage. This blastomere generates columns 3 and 4 of the A-line neural plate as well as one quarter of the A-line notochord, a trunk lateral cell and an endoderm precursor. This procedure resulted in the loss of *Ci-MRF* expression and ectopic *Ci-COE* expression in row I, phenocopying UO126 treatment from the early gastrula stage (Fig. 7D). Although we cannot rule out that the transformation of neural plate cells is a secondary effect of mis-specification of the other tissue precursors derived from A5.2, these data support a role for FGF signalling during the differential specification of row I and row II cells.

Taken together, these results suggest that an FGF signal is required for ERK activation in row I cells, which acts to promote row I fates and repress row II fates, patterning the caudal neural plate along the anteroposterior axis.

Table 1. Expression of row I and row II markers following UO126 treatment from the early gastrula stage

		Control			UO126		
		%	Mean	*n*	%	Mean	*n*
Ci-MRF		99	1.9	159	2	0.0	64
Ci-Tbx6b		84	1.5	57	0	0.0	50
Ci-Actin		98	1.7	54	0	0.0	59
Ci-ephrinAb		92	1.6	103	2.5	0.0	119
Ci-Mnx		99	3.9	130	3	0.1	115
Ci-Cdx		100	5.3	79	0	0.0	110
Ci-COE	Row I	13	0.2	108	99	1.9	69
	Row II	98	1.6		100	1.8	
Ci-FGF8/17/18	Row I	1	0.1	135	95	1.9	110
	Row II	93	1.8		99	1.8	
Ci-FGF9/16/20	Row I	0	0.0	129	80	3.0	127
	Row II	99	3.7		100	4	
cicl007j15	Row I	5	0.1	137	66	1.8	86
	Row II	100	3.6		100	3.5	

Expression in row I was counted for row I markers (*Ci-MRF*, *Ci-Tbx6b*, *Ci-Actin*, *Ci-ephrinAb*, *Ci-Mnx*, *Ci-Cdx*), and in row I and row II for row II markers (*Ci-COE*, *Ci-FGF8/17/18*, *Ci-FGF9/16/20*, *cicl007j15*). %, percentage of embryos showing any expression; Mean, mean number of neural plate cells positive for each marker; *n*, total number of embryos analysed.

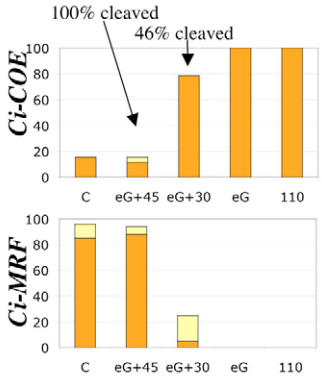

Fig. 8. Expression of *Ci-COE* and *Ci-MRF* following UO126 treatment at different time points. Graphs show the percentage of embryos showing expression in A9.31 (row I/column 4). The key for the graph and scoring is the same as in Fig. 5. A sample of embryos was taken at the same time point that embryos were placed in inhibitor and analysed for *Ci-Ngn* expression to determine the percentage of embryos in each sample in which A8.16 had cleaved. These percentages are indicated on the graphs (arrows). On the *x*-axis: C, control; 110, 110-cell stage; eG, early gastrula stage; eG+30, 30 minutes after eG; eG+45, 45 minutes after eG. The minimum number of embryos analysed for each time point was 12 embryos for *Ci-COE* and 17 for *Ci-MRF*. This experiment was repeated two more times with similar results (data not shown).

DISCUSSION

We have shown that three distinct signalling pathways are integrated during patterning of the A-line neural plate and play a major role in establishing a grid-like pattern of gene expression domains (Fig. 9). Nodal signals are required for all lateral neural plate fates and to restrict medial fates, early Delta2/Notch is required for column 4 fates, late Delta2/Notch is required for column 2 fates, and FGF/MEK/ERK is required to promote row I fates and restrict row II fates. Each neural plate precursor receives a distinct combination of the three signalling pathways, which are required to define each of the eight cell types (Fig. 9). For example, the formation of the

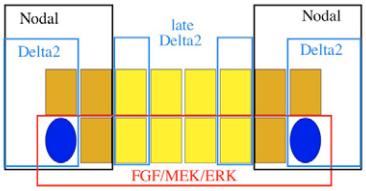

Fig. 9. Summary of the overlapping requirements of Nodal, Delta2 and FGF/MEK/ERK signalling pathways in the A-line neural plate.

secondary muscle precursor in the row I/column 4 position requires positive input from all three signalling pathways. These signalling pathways appear to be acting sequentially. *Nodal* expression begins at the 32-cell stage and the Nodal-mediated medial versus lateral fate choice is achieved around the 64- to 76-cell stage. Nodal signalling is required for the specification of all derivatives of A7.8 (founder cell of columns 3 and 4), which emerges at the 64-cell stage. *Delta2*, a transcriptional target of Nodal signalling, is expressed from the late 64-cell stage and is required for fate specification of A8.16 (precursor of column 4), which forms at the 76-cell stage. Later, at around the 110-cell stage, Ci-Delta2 is expressed in cells adjacent to column 2 precursors and is required to promote column 2 and repress column 1 identity. Finally, FGF/ERK activation in row I but not in row II cells at neural plate stages is required for the differential fate specification between these two rows of cells. It is likely that the molecules used as markers in this study are also interacting with each other. For example, it has been shown that *Ci-Snail*, which is expressed in the lateral neural cells and is activated by Nodal, is required for repression of the medial marker *Ci-Mnx* (Imai et al., 2006).

We previously noted that mediolateral patterning of the A-line neural plate appeared to be independent of anteroposterior patterning, because the expansion of medial marker expression observed following Nodal inhibition remained in the correct row of cells (Fig. 2) (Hudson and Yasuo, 2005). In support of this, here we show that disruption of anteroposterior patterning by FGF/MEK/ERK inhibition from the early gastrula stage resulted in adoption of row II-like fates in row I in manner respecting columnar position (Fig. 7). Thus, mediolateral and anteroposterior patterning of the neural plate are uncoupled, independent events.

Nodal, Delta2 and FGF/MEK/ERK signalling during neural tube patterning of *Ciona*

Laterally localised Nodal signals provide a positional cue, which initiates patterning along the mediolateral axis of the posterior neural plate. This pattern is achieved through an alternative fate choice, with Nodal promoting lateral and repressing medial identity, and results in the subdivision of the neural plate precursors into two domains, a *Ci-Snail/Ci-Delta2*-positive lateral domain and a *cicl007j15*-positive medial domain (this study) (Hudson and Yasuo, 2005). Nodal signalling is also required for lateral neural plate fates in the anterior (a-line) neural plate and for expression of markers in b-line neural precursors (Hudson and Yasuo, 2005; Imai et al., 2006). Further work will be required to understand whether these anterior neural cells adopt alternative fates in the absence of Nodal signals.

In the posterior neural plate, Delta2 refines the initial pattern established by Nodal. During the specification of column 4 fates, Delta2/Notch signals do not appear to be driving a binary cell fate switch, because column 4 cells do not adopt their column 3 sister cell

identity following Delta2/Notch signal inhibition. Continued expression of general lateral neural plate markers (*Ci-Snail*, *Ci-Delta2*, *Ci-Chordin*) throughout the lateral neural plate indicates that column 4 cells retain lateral neural identity (Figs 4, 5). However, only rarely was ectopic expression of the column 3 markers *Ci-ephrinAb* and *Ci-FGF8/17/18* observed in column 4 (Fig. 5). This suggests that other mechanisms might operate in the embryo to repress column 3 fates in column 4. Alternatively, there might be additional signals required to induce column 3 fates in column 3. One possible candidate is BMP2/4, which has been shown in *Halocynthia* to be required for specification of motoneurons, which are column 3 derivatives (Katsuyama et al., 2005). In addition to column 4 specification, we have found that later Delta2/Notch signals are implicated in the formation of column 2 versus column 1 identity. In this case, the Delta2/Notch signal might act as a binary switch, because column 1 fates are ectopically expressed in column 2 following Delta2/Notch signal disruption.

Superimposed on this mediolateral pattern is a difference in anteroposterior identities established by the differential activation of ERK1/2 between rows I and II (Fig. 7). We show that this differential fate specification requires FGF-signalling within the A5.2 lineage. Within the a-line neural plate, ERK1/2 is also differentially activated between the row III (active) and row IV (inactive) sister rows (Fig. 7). Thus, in both A- and a-lineages, ERK1/2 activity is associated with the posterior-most row of cells. Further studies will be required to establish whether row III fates adopt row IV fates in the absence of FGF/MEK/ERK activity.

It will be important in future studies to reveal the ultimate fates of each of these neural plate cells by precise fate mapping coupled with marker analysis, and to verify whether the early changes in neural plate patterning described in this study manifest as terminal fate changes in the CNS.

Nodal, Notch and MEK/ERK signalling during vertebrate neural patterning

All three of these signalling pathways are involved in a myriad of cell fate specification events during vertebrate development. Within the vertebrate neural tube, Nodal is required for induction of the floor plate, the ventral-most structure of the neural tube, at least in zebrafish (reviewed in Strähle et al., 2004). This is at odds with the role for Nodal in promoting lateral fates at the expense of medial (including floor plate) fates in ascidians and suggests that the role of Nodal in neural tube patterning is not conserved among chordates. By contrast, in the vertebrate neural tube, Delta/Notch signalling has been implicated in the formation of both extreme dorsal (neural crest) and ventral (floor plate) cell types (Cornell and Eisen, 2005; Latimer and Appel, 2006). In *Ciona*, Delta2/Notch is involved in both the specification of lateral and medial fates within the neural plate. Interestingly, there are some differences in the mode of action of Delta/Notch signalling in *Ciona*, because *Ci-MRF*, *Ci-COE* and *Ci-Ngn*, which all encode HLH proteins, are activated by Delta2/Notch, whereas expression of these transcription factors is generally negatively regulated by Notch signals (e.g. Dubois and Vincent, 2001; Hansson et al., 2004; Kuroda et al., 1999; Ma et al., 1996; Umbhauer et al., 2001; Wittenberger et al., 1999). Later, during neurogenesis, Notch signalling is involved in the selection of neurones in neurogenic regions of the developing neural plate, a process known as lateral inhibition (reviewed in Lai, 2004). Although this role has not been addressed in the CNS of *Ciona*, it is involved in the selection of epidermal sensory neurones within the dorsal and ventral midline neurogenic regions of the larval tail epidermis (Pasini et al., 2006).

In vertebrates, FGF, together with Wnt, signalling is required during late gastrula stages to impose a posterior identity on neural tissue (e.g. Gamse and Sive, 2000; Nordström et al., 2006). This is reminiscent of the situation in ascidians, in which we have shown that FGF/MEK/ERK signalling is required for posterior identities in the neural plate. Thus, the role of this signalling pathway during posteriorisation might represent a core evolutionary strategy to generate posterior cell types within neural tissue.

Concluding remarks

The simple organisation of the ascidian neural plate allows us to understand cell fate diversification at the level of individual cells. Our studies have enabled us to superimpose the activity of three overlapping signalling pathways onto the grid-like organisation of cells and gene expression patterns in the neural plate (Fig. 9). It will be imperative in future studies to try to understand how these signalling pathways are integrated at the level of transcriptional control of cell-type-specific gene markers, particularly in the lateral neural plate, in which a specific marker for each individual cell has been identified. Taken together with recent advances in establishing gene regulatory networks during early *Ciona* development (Imai et al., 2006), it is not unreasonable to expect that it will ultimately be possible to establish a gene regulatory network, integrating cell signalling and transcription factor inputs, for each individual cell of the neural plate.

We thank N. Satoh and colleagues for kindly providing the *Ciona* Gene Collection plates; T. Meedel for sharing data on the expression pattern of *Ci-MRF* prior to publication; A. Pasini for the kind gift of the FOG::Delta2 construct; and E. Houliston and A. Pasini for critical reading of the manuscript. Thank you also to the staff of the UMR7009 for their many kinds of help and support. This work was funded by the Centre National de la Recherche Scientifique (CNRS), the Université Paris VI, the Association Française contre les Myopathies (AFM; grant nos 9960 and 11734), the Association pour la Recherche sur le Cancer (ARC, grant no. 3885) and the Agence Nationale de la Recherche (ANR).

Supplementary material

Supplementary material for this article is available at http://dev.biologists.org/cgi/content/full/134/19/3527/DC1

References

Bertrand, V., Hudson, C., Caillol, D., Popovici, C. and Lemaire, P. (2003). Neural tissue in ascidian embryos is induced by FGF9/16/20, acting via a combination of maternal GATA and Ets transcription factors. *Cell* **115**, 615-627.

Cole, A. G. and Meinertzhagen, I. A. (2004). The central nervous system of the ascidian larva: mitotic history of cells forming the neural tube in late embryonic Ciona intestinalis. *Dev. Biol.* **271**, 239-262.

Conklin, E. G. (1905). The organisation and cell lineage of the ascidian egg. *J. Acad. Nat. Sci. Philadelphia* **13**, 1-119.

Corbo, J. C., Levine, M. and Zeller, R. W. (1997). Characterization of a notochord-specific enhancer from the Brachyury promoter region of the ascidian, Ciona intestinalis. *Development* **124**, 589-602.

Cornell, R. A. and Eisen, J. S. (2005). Notch in the pathway: the roles of Notch signaling in neural crest development. *Semin. Cell Dev. Biol.* **16**, 663-672.

Dehal, P., Satou, Y., Campbell, R. K., Chapman, J., Degnan, B., De Tomaso, A., Davidson, B., Di Gregorio, A., Gelpke, M., Goodstein, D. M. et al. (2002). The draft genome of Ciona intestinalis: insights into chordate and vertebrate origins. *Science* **298**, 2157-2167.

Dubois, L. and Vincent, A. (2001). The COE–Collier/Olf1/EBF–transcription factors: structural conservation and diversity of developmental functions. *Mech. Dev.* **108**, 3-12.

Dufour, H. D., Chettouh, Z., Deyts, C., de Rosa, R., Goridis, C., Joly, J. S. and Brunet, J. F. (2006). Precraniate origin of cranial motoneurons. *Proc. Natl. Acad. Sci. USA* **103**, 8727-8732.

Duncia, J. V., Santella, J. B., 3rd, Higley, C. A., Pitts, W. J., Wityak, J., Frietze, W. E., Rankin, F. W., Sun, J. H., Earl, R. A., Tabaka, A. C. et al. (1998). MEK inhibitors: the chemistry and biological activity of U0126, its analogs, and cyclization products. *Bioorg. Med. Chem. Lett.* **8**, 2839-2844.

Favata, M. F., Horiuchi, K. Y., Manos, E. J., Daulerio, A. J., Stradley, D. A., Feeser, W. S., Van Dyk, D. E., Pitts, W. J., Earl, R. A., Hobbs, F. et al. (1998).

Identification of a novel inhibitor of mitogen-activated protein kinase kinase. *J. Biol. Chem*. **273**, 18623-18632.
Fujiwara, S., Maeda, Y., Shin-I, T., Kohara, Y., Takatori, N., Satou, Y. and Satoh, N. (2002). Gene expression profiles in Ciona intestinalis cleavage-stage embryos. *Mech. Dev*. **112**, 115-127.
Gamse, J. and Sive, H. (2000). Vertebrate anteroposterior patterning: the Xenopus neurectoderm as a paradigm. *BioEssays* **22**, 976-986.
Geling, A., Steiner, H., Willem, M., Bally-Cuif, L. and Haass, C. (2002). A gamma-secretase inhibitor blocks Notch signaling in vivo and causes a severe neurogenic phenotype in zebrafish. *EMBO Rep*. **3**, 688-694.
Hansson, E. M., Lendahl, U. and Chapman, G. (2004). Notch signaling in development and disease. *Semin. Cancer Biol.* **14**, 320-328.
Hudson, C. and Lemaire, P. (2001). Induction of anterior neural fates in the ascidian Ciona intestinalis. *Mech. Dev*. **100**, 189-203.
Hudson, C. and Yasuo, H. (2005). Patterning across the ascidian neural plate by lateral Nodal signalling sources. *Development* **132**, 1199-1210.
Hudson, C. and Yasuo, H. (2006). A signalling relay involving Nodal and Delta ligands acts during secondary notochord induction in *Ciona* embryos. *Development* **133**, 2855-2864.
Hudson, C., Darras, S., Caillol, D., Yasuo, H. and Lemaire, P. (2003). A conserved role for the MEK signalling pathway in neural tissue specification and posteriorisation in the invertebrate chordate, the ascidian Ciona intestinalis. *Development* **130**, 147-159.
Imai, K. S., Satoh, N., Satou, Y. (2002). Early embryonic expression of FGF4/6/9 gene and its role in the induction of mesenchyme and notochord in *Ciona savignyi* embryos. *Development* **129**, 1729-1738.
Imai, K. S., Hino, K., Yagi, K., Satoh, N. and Satou, Y. (2004). Gene expression profiles of transcription factors and signaling molecules in the ascidian embryo: towards a comprehensive understanding of gene networks. *Development* **131**, 4047-4058.
Imai, K. S., Levine, M., Satoh, N. and Satou, Y. (2006). Regulatory blueprint for a chordate embryo. *Science* **312**, 1183-1187.
Inman, G. J., Nicolas, F. J., Callahan, J. F., Harling, J. D., Gaster, L. M., Reith, A. D., Laping, N. J. and Hill, C. S. (2002). SB-431542 is a potent and specific inhibitor of transforming growth factor-beta superfamily type I activin receptor-like kinase (ALK) receptors ALK4, ALK5, and ALK7. *Mol. Pharmacol.* **62**, 65-74.
Katsuyama, Y., Okada, T., Matsumoto, J., Ohtsuka, Y., Terashima, T. and Okamura, Y. (2005). Early specification of ascidian larval motor neurons. *Dev. Biol*. **278**, 310-322.
Kuroda, K., Tani, S., Tamura, K., Minoguchi, S., Kurooka, H. and Honjo, T. (1999). Delta-induced Notch signaling mediated by RBP-J inhibits MyoD expression and myogenesis. *J. Biol. Chem*. **274**, 7238-7244.
Lai, E. C. (2004). Notch signaling: control of cell communication and cell fate. *Development* **131**, 965-973.
Latimer, A. J. and Appel, B. (2006). Notch signalling regulates midline cell specification and proliferation in zebrafish. *Dev. Biol*. **298**, 392-402.
Lemaire, P., Bertrand, V. and Hudson, C. (2002). Early steps in the formation of neural tissue in ascidian embryos. *Dev. Biol*. **252**, 151-169.
Ma, Q., Kintner, C. and Anderson, D. J. (1996). Identification of neurogenin, a vertebrate neuronal determination gene. *Cell* **87**, 43-52.
Meedel, T. H., Chang, P. and Yasuo, H. (2007). Muscle development in Ciona intestinalis requires the b-HLH myogenic regulatory factor gene Ci-MRF. *Dev. Biol*. **302**, 333-344.
Moret, F., Christiaen, L., Deyts, C., Blin, M., Vernier, P. and Joly, J. S. (2005). Regulatory gene expressions in the ascidian ventral sensory vesicle: evolutionary relationships with the vertebrate hypothalamus. *Dev. Biol*. **277**, 567-579.
Nicol, D. and Meinertzhagen, I. A. (1988a). Development of the central nervous system of the larva of the ascidian, Ciona intestinalis L. I. The early lineages of the neural plate. *Dev. Biol.* **130**, 721-736.
Nicol, D. and Meinertzhagen, I. A. (1988b). Development of the central nervous system of the larva of the ascidian, Ciona intestinalis L. II. Neural plate morphogenesis and cell lineages during neurulation. *Dev. Biol.* **130**, 737-766.
Nishida, H. (1987). Cell lineage analysis in ascidian embryos by intracellular injection of a tracer enzyme. III. Up to the tissue restricted stage. *Dev. Biol.* **121**, 526-541.
Nishida, H. (1990). Determinative mechanisms in secondary muscle lineages of ascidian embryos: development of muscle-specific features in isolated muscle progenitor cells. *Development* **108**, 559-568.
Nishida, H. (2003). Spatio-temporal pattern of MAP kinase activation in embryos of the ascidian Halocynthia roretzi. *Dev. Growth Differ*. **45**, 27-37.
Nordström, U., Maier, E., Jessell, T. M. and Edlund, T. (2006). An early role for Wnt signaling in specifying neural patterns of Cdx and Hox gene expression and motor neuron subtype identity. *PLoS Biol*. **4**, e252.
Pasini, A., Amiel, A., Rothbacher, U., Roure, A., Lemaire, P. and Darras, S. (2006). Formation of the ascidian epidermal sensory neurons: insights into the origin of the chordate peripheral nervous system. *PLoS Biol.* **4**, e225.
Picco, V., Hudson, C. and Yasuo, H. (2007). Ephrin/Eph signalling drives the asymmetric division of notochord/neural precursors in Ciona embryos. *Development* **134**, 1491-1497.
Satou, Y., Sasakura, Y., Yamada, L., Imai, K. S., Satoh, N. and Degnan, B. (2003a). A genomewide survey of developmentally relevant genes in Ciona intestinalis. V. Genes for receptor tyrosine kinase pathway and Notch signaling pathway. *Dev. Genes Evol*. **213**, 254-263.
Satou, Y., Imai, K. S., Levine, M., Kohara, Y., Rokhsar, D. and Satoh, N. (2003b). A genomewide survey of developmentally relevant genes in Ciona intestinalis. I. Genes for bHLH transcription factors. *Dev. Genes Evol*. **213**, 213-221.
Satou, Y., Kawashima, T., Shoguchi, E., Nakayama, A. and Satoh, N. (2005). An integrated database of the ascidian, Ciona intestinalis: towards functional genomics. *Zool. Sci*. **22**, 837-843.
Strähle, U., Lam, C. S., Ertzer, R. and Rastegar, S. (2004). Vertebrate floor-plate specification: variations on common themes. *Trends Genet*. **20**, 155-162.
Takatori, N., Hotta, K., Mochizuki, Y., Satoh, G., Mitani, Y., Satoh, N., Satou, Y. and Takahashi, H. (2004). T-box genes in the ascidian Ciona intestinalis: characterization of cDNAs and spatial expression. *Dev. Dyn*. **230**, 743-753.
Tassy, O., Daian, F., Hudson, C., Bertrand, V. and Lemaire, P. (2006). A quantitative approach to the study of cell shapes and interactions during early chordate embryogenesis. *Curr. Biol.* **16**, 345-358.
Umbhauer, M., Boucaut, J. C. and Shi, D. L. (2001). Repression of XMyoD expression and myogenesis by Xhairy-1 in Xenopus early embryo. *Mech. Dev*. **109**, 61-68.
Wada, S., Katsuyama, Y., Yasugi, S. and Saiga, H. (1995). Spatially and temporally regulated expression of the LIM class homeobox gene Hrlim suggests multiple distinct functions in development of the ascidian, Halocynthia roretzi. *Mech. Dev.* **51**, 115-126.
Wittenberger, T., Steinbach, O. C., Authaler, A., Kopan, R. and Rupp, R. A. (1999). MyoD stimulates delta-1 transcription and triggers notch signaling in the Xenopus gastrula. *EMBO J.* **18**, 1915-1922.
Yasuo, H. and Hudson, C. (2007). FGF8/17/18 functions together with FGF9/16/20 during formation of the notochord in *Ciona* embryos. *Dev. Biol.* **302**, 92-103.